Fusion Engineering and Design 154 (2020) 111537

Contents lists available at ScienceDirect

Fusion Engineering and Design

journal homepage: www.elsevier.com/locate/fusengdes

Real-time gas cooling of flowing liquid lithium limiter for the EAST

X.C. Meng[a,b,1], M. Huang[c,1], C.L. Li[c], Z. Sun[d], W. Xu[a,b], R. Maingi[d], K. Tritz[e], D. Andruczyk[f], Y.Z. Qian[c], Q.X. Yang[c], X.L. Yuan[c], J.J. Huang[a], X. Gao[c], B. Yu[b], J.G. Li[c], G.Z. Zuo[c,*], J.S. Hu[c,g,*], EAST team[2]

[a] Advanced Energy Research Center, Shenzhen University, Shenzhen 518060, China
[b] Key Laboratory of Optoelectronic Devices and Systems of Ministry of Education and Guangdong Province, College of Optoelectronic Engineering, Shenzhen University, Shenzhen 518060, China
[c] Institute of Plasma Physics, Chinese Academy of Sciences, Hefei 230031, China
[d] Plasma Physics Laboratory, Princeton University, Princeton, NJ 08543, USA
[e] Johns Hopkins University, Baltimore, MD 21211, USA
[f] Center for Plasma Material Interactions, Department of Nuclear, Plasma and Radiological Engineering, University of Illinois Urbana-Champaign, Urbana IL, 61801, USA
[g] CAS Key Laboratory of Photovoltaic and Energy Conservation Materials, Hefei, 230031, China

ARTICLE INFO

Keywords:
Gas cooling
Liquid lithium limiter
Heat flux
Plasma

ABSTRACT

A novel continuously flowing liquid lithium limiter (FLiLi) which employs an in-vessel electro-magnetic pump to drive liquid Li flowing on the surface of limiter has been successfully designed and tested in the experimental advanced superconducting tokamak (EAST) device in 2014. In order to better control the surface temperature, an upgraded design and the real-time gas cooling were performed in 2016. Two kinds of cooling gas, helium (He) and argon (Ar) were tested on the FLiLi system prior to the experiment. It was found that the cooling rates of He and Ar at 2.5 MPa are 34.2 ℃/min, 10.2 ℃/min or 31.7 ℃/kL and 28.1 ℃/kL, respectively. The cooling performance of He is more effective than Ar. Experimental results show that the real-time He cooling could effectively contain the FLiLi surface temperature increase and prevent the strong passive evaporation of lithium during plasma discharges. Limiter heat flux up to 0.2 MW/m^2 was removed during ohmic discharge with 2.5 MPa He gas. Finally, Because of the upgraded design and real-time gas cooling, the surface of FLiLi was not damaged by heat flux after entire plasma discharge.

1. Introduction

Traditional plasma facing materials (PFMs) currently suffer from several issues due to the intense plasma surface interaction (PSI) [1,2]. These include melting, cracking and atomic displacement with in the lattice of the materials which can significantly change the structural and thermal properties of the material and surface. As an alternative to solid PFMs, liquid lithium (Li) has a reasonable heat removal capacity, excellent compatibility with plasma due to its low-z nature, and a wide temperature range in the liquid state; additionally, liquid Li can pump hydrogenic and impurity species, which can be used for effective particle control. Using liquid Li as a PFM has been tested in many tokamaks, with good signs of plasma performance improvement [3–7]. Particularly, flowing liquid lithium can also offer a self-healing surface during plasma discharges [8]. Liquid Li used as a plasma facing components (PFC) can be attractive for future fusion devices.

In 2014, based on the concept of a thin flowing film, a novel, continuously flowing liquid Li limiter (FLiLi), which used an in-vessel direct current (DC) electromagnetic (EM) pump and the steady-state toroidal magnetic field of the EAST device to drive liquid Li in closed recirculation loop on the limiter surface, was successfully designed and tested in EAST [9,10]. It was found that the FLiLi was fully compatible with high performance plasmas. During the experiment, a circulating Li layer with a thickness of < 1 mm and a flow rate $\sim$ 2cm^3s^{-1} was achieved by adjusting the applied DC current of the EM pump. Moreover, the recycling, impurities and divertor heat flux were reduced, and the plasma stored energy increased by using FLiLi [9,11]. This FLiLi used a 0.1 mm thick stainless steel (SS) coating to prevent contact between the liquid Li and Cu heat sink. Nevertheless, after the conclusion of the experiment, the surface of the FLiLi was damaged due to PSI, and

* Corresponding authors at: Institute of Plasma Physics, Chinese Academy of Sciences, Hefei 230031, China.
E-mail addresses: zuoguizh@ipp.ac.cn (G.Z. Zuo), hujs@ipp.ac.cn (J.S. Hu).
[1] Co-first author.
[2] Plasma operation.

https://doi.org/10.1016/j.fusengdes.2020.111537
Received 25 July 2019; Received in revised form 15 January 2020; Accepted 4 February 2020

Fig. 1. The picture of FLiLi surface after exposing to air in 2014.

that the Cu heat sink was exposed and damaged by liquid Li [12], as shown in Fig. 1. Hence, it is necessary to better control surface temperature of FLiLi during plasma discharge.

In order to enhance the surface erosion resistance for the second-generation FLiLi, an upgraded design with several technological improvements were applied in December 2016. First, the thickness of the SS protective surface layer of FLiLi was increased from 0.1 mm to 0.5 mm. Second, to improve the thermal contact between the underlying Cu heat sink and the SS layer, Hot Isostatic Pressing (HIP) technology was applied [13]. Finally, real-time gas cooling was used in 2016 campaign. In this paper, the real-time gas cooling of FLiLi for improving the surface erosion resistance in EAST is presented. The experimental layout of the gas cooling capacity test is introduced in Section 2. The results of gas cooling capacities and the cooling effect of He on the FLiLi during plasma discharges is given in Section 3. Finally, the conclusions drawn from the experiments are documented in Section 4.

2. Experimental setup and procedures

2.1. FLiLi system

As shown in the Fig. 2, the second-generation FLiLi plate is composed of a Cu plate with a length of 320 mm and width of 300 mm. Three heating cartridges are deployed on the upper and lower ends of the Cu plate. To cool the limiter, two cooling tubes, an inlet and an outlet, are brazed on back of the plate. These cooling lines are arranged in the middle of the Cu plate because the main contact area between the plasma and limiter is on middle of the FLiLi. As shown by the green dots of Fig. 2(b), 12 thermocouples are evenly attached to the Cu plate for measuring the limiter temperature distribution. In addition, two thermocouples are also mounted on the surface of distributor and collector box respectively. The control system of FLiLi in 2016 was the same as that used in 2014 [14].

A specific sequence of actions is required to implement FLiLi on EAST. First, the FLiLi was assembled in the Li and Plasma Evaluation System (LiPES) in laboratory [15]. Then, as shown in Fig. 3, the entire assembled system of LiPES was moved and installed at the H port on EAST, including a limiter head, a filling system, an exchange box, a limiter driving system, heating and cooling systems, and a control system. Note that the cooling system includes gas cylinders, flowmeter, inlet pipe, cooling line, vent pipe and temperature monitoring system.

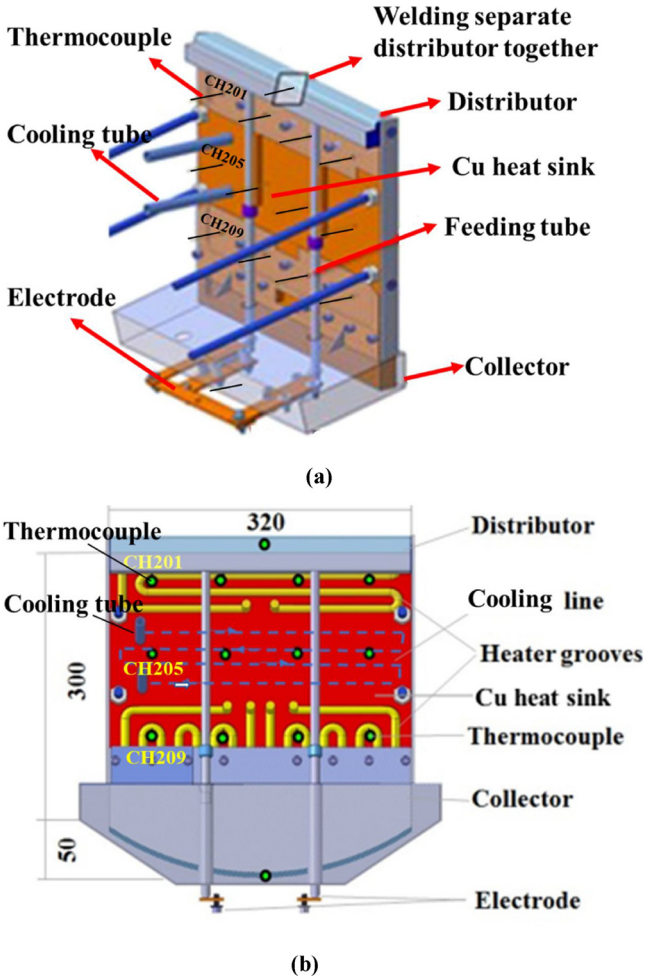

Fig. 2. Schematic diagram of FLiLi. s (a) 3D side view of FLiLi, (b) back structure of FLiLi.

2.2. Experimental procedures

There are several choices that could have been used for the coolant for FLiLi. The coolant should have high specific heat capacity, high security, and easy and affordable availability. Although water has a high specific heat capacity at room temperature, it is not a good choice for the FLiLi coolant because it can easily react with liquid Li and release large amount of heat and hydrogen. Studies have shown that 22.58 kPa of pressure can released in a few microseconds, followed by 21 kPa of pressure in a few seconds when 0.5 g of 300 ℃ liquid Li reacts with 30 ℃ water [16]. In FLiLi experiment, there were about 600 g of high temperature liquid Li in the collector box. Hence, we opted to use gas as the coolant in this experiment for safety reasons. During fusion device vacuum testing and vessel bake-out, hot N_2 is also commonly used, e.g. to heat the PFCs to a sufficient temperature to drive out water vapor and other residual gases [17]. However, Li is readily reactive with N_2 to form Li_3N. The following reaction is well known:

$$\text{Li (l)} + 1/6\ \text{N}_2\ \text{(g)} \rightarrow 1/3\text{Li}_3\text{N (s)} - 69\ \text{kJ/g·mol Li (414 kJ/g·mol N}_2\text{, at 500 °C).} \quad (1)$$

Furthermore, the character of Li interaction with N_2 is mainly determined by the solubility of N_2 in Li. Specifically the nonmetallic impurity solubility in lithium depends on the temperature range [18]:

$$\ln C = A - BT^{-1}, \quad (2)$$

where C is the concentration of an impurity in liquid metal in atomic fraction, %; T is temperature in K, A and B are constants. For N_2, the A

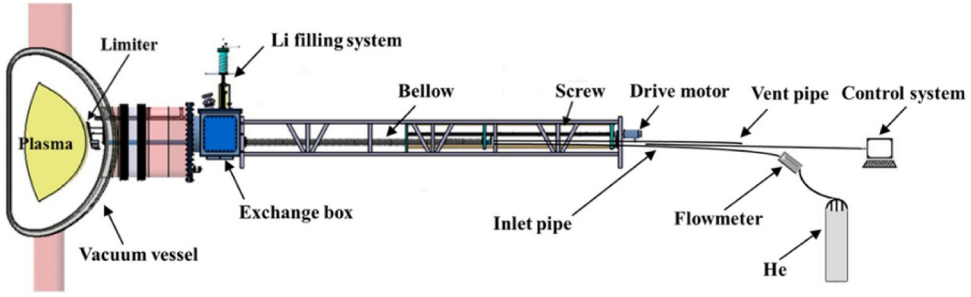

Fig. 3. The FLiLi system on EAST.

and B are 7.581 and 4832 respectively for Li temperature at 300 ℃ (573 K). The concentration of N_2 in 300 ℃liquid Li is about 0.43 %. Hence, N_2 possesses a high solubility in high temperature liquid Li. Thus, it is unsuitable to use N_2 as a coolant of FLiLi. Ar is an inert gas which does not react with Li, and it is commonly used for vacuum maintenance in EAST. Finally, Liquid He is a candidate coolant for superconducting coils and blanket in fusion device. Moreover, He is an intrinsic fusion by-product, and it does not react with Li too. Therefore, we chose to test He and Ar gas as the FLiLi coolant.

Prior to FLiLi operation, the limiter was pushed into the vacuum vessel of EAST via a stepper motor drive; the limiter was then heated up to ~400 ℃ for 12 h for outgassing. Then the cooling effectiveness of the three gases Ar and He were tested. The procedure for e.g. Ar testing is now described. First, adjusting Ar pressure to 2.5 MPa through the regulator valve; note that flowmeter has a maximum pressure of 3 MPa. Then, the time for the limiter temperature to drop from 400 ℃ to 200 ℃ for a given Ar flow rate was determined. Finally, the Ar flow was terminated and the limiter re-heat time back to 400 ℃ was recorded. After testing, the gas of He and Ar with the best cooling effect was selected as the coolant in the FLiLi experiment during plasma discharge.

3. Results and discussion

As seen in Fig. 2, the thermocouple corresponding to channel 205, which is located in middle of the Cu plate, is closest to the cooling pipe. It can be assumed that this thermocouple should have the fastest response to cooling. Therefore, channel 205 was selected for feedback control. During the cooling test, the time and gas quantity required for FLiLi surface temperature to drop from 303 ℃ to 230 ℃ under different gas cooling conditions were measured, as shown in Fig. 4. It can be seen that He takes significantly less time to cool the limiter than Ar. The cooling rates of He and Ar are 34.2 ℃/s and 10.2 ℃/s respectively. The required quantities of these three gases for cooling are also comparable. The cooling rates of He and Ar can also be expressed as 31.7 ℃/kL and 28.1 ℃/kL.

In addition, the cooling performance for H and Ar were simulated by ANSYS. It was assumed that the FLiLi surface temperature is uniform and the initial temperature was 400 ℃. Then the temperature distribution was simulated 15 s after three different gases were applied at 25℃ and 2.5 MPa. Fig. 5 shows the 2D simulation results of FLiLi surface temperature distribution. The results also indicated that the cooling effect of He is better than Ar which gives good agreement with the experimental results.

In view of the above results, He is the most suitable coolant for FLiLi experiments during plasma discharge. Fig. 6 compares two typical ohmic plasmas with identical plasma current and density, but with different surface temperature of FLiLi during/after plasma discharge with/without high pressure He cooling (shot #71355, black traces; shot #71356, red traces; ohmic heating only, $I_p = 0.4$ MA; $n_e \sim 2.6 \times 10^{19}\,m^{-3}$). FLiLi located in the same radial position (R = 2.305 m) during shots #71355 #71356.

As mentioned above, we select the data of channel 205 to analyze

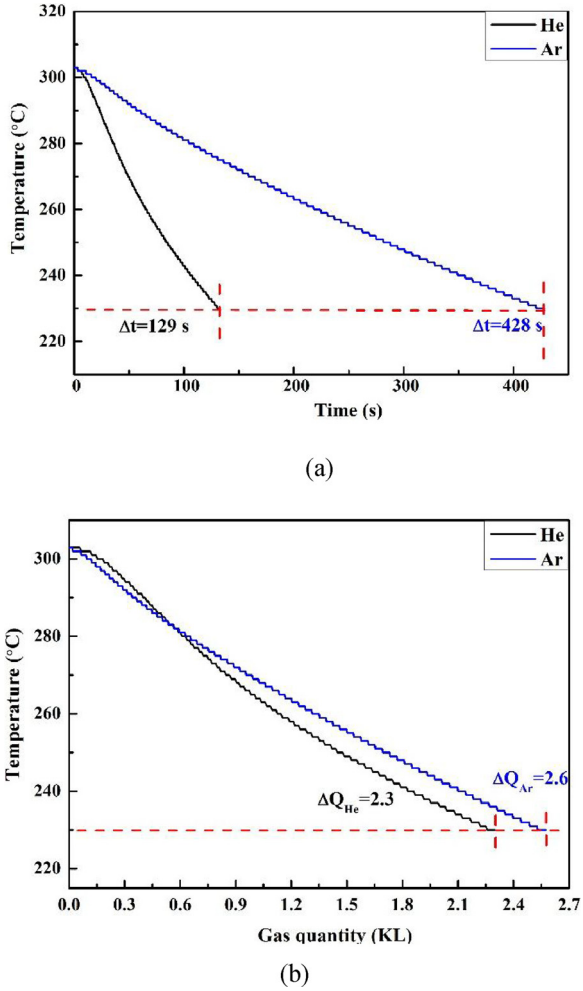

Fig. 4. Temperature evolution of channel 205. (a) Temperature curve over time, (b) temperature curve over gas quantity.

the cooling effect of He on FLiLi surface during plasma discharges. Fig. 7 shows the temperature evolution of channel 205 during discharges of shots #71355 and #71356. Without He cooling, the temperature continuously increased with time during shot #71355. During shot #71356, He gas reduced the temperature ramp rate, and the temperature quickly reached its maximum value and fell rapidly at 20 s. The maximum temperature rises of shots #71355 and #71356 after plasma discharges were 29 and 20 ℃ respectively, with a ΔT ~ 9 ℃. The result confirms that the design of FLiLi gas cooling system could operate successfully during plasma discharges.

The temperature rise of PFMs is mainly caused by the plasma heat flux. The temperature rises on the FLiLi surface under a heat flux q (t), can be written as [19]:

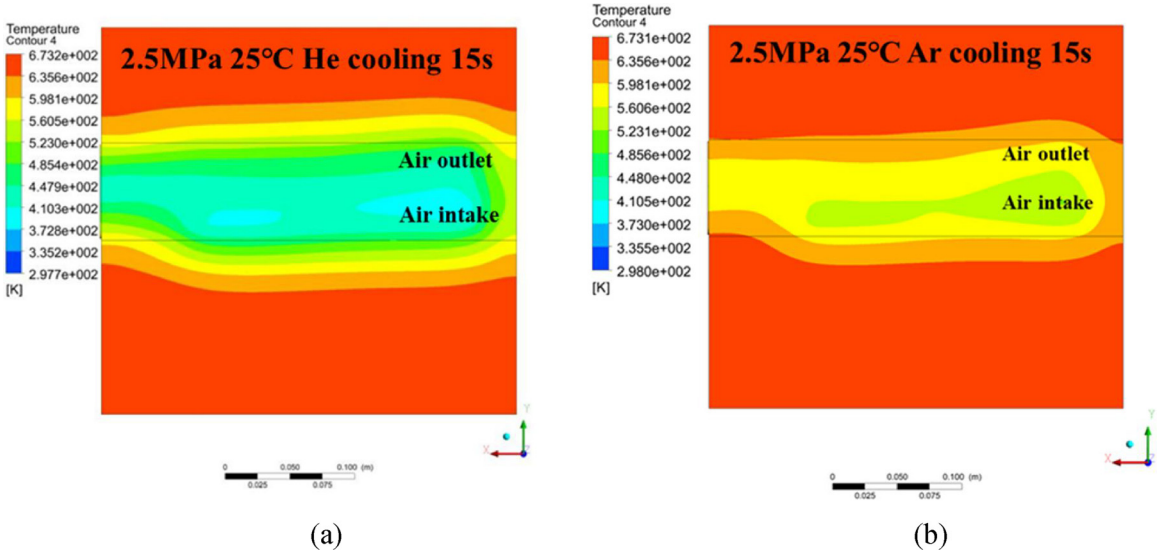

Fig. 5. 2D simulation results of FLiLi surface temperature distribution with different gases.

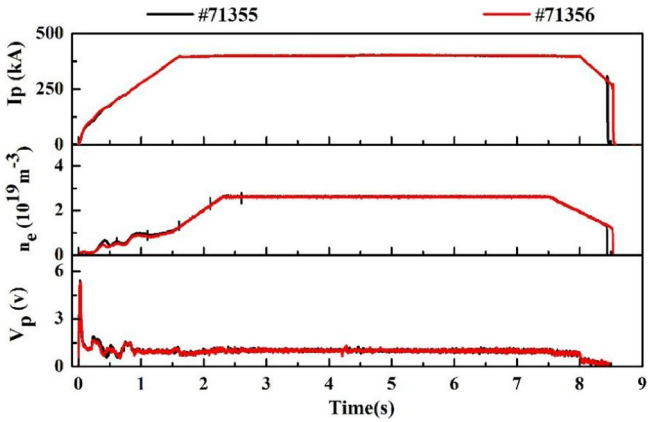

Fig. 6. Plasma parameters of shots #71355 and #71356.

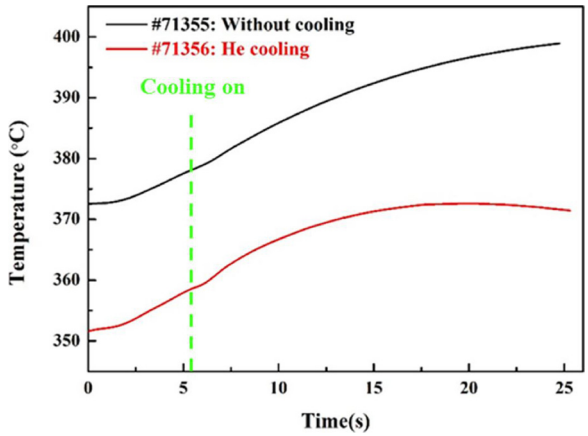

Fig. 7. Comparison of temperature evolution during shots #71355 and shot #71356.

$$\Delta T(t) = 1/\sqrt{\pi\rho ck}\int_0^t q(t-t')/\sqrt{t'}\,dt' \tag{3}$$

where T and q are limiter temperature and heat flux respectively. Here ρ is density of material, t is time elapsed since initial exposure of the plasma heat flux, c is specific heat capacity of limiter material, and k is heat conductivity coefficient [20]. To simplify the calculation, it is assumed that the q is a constant. The Eq. (3) can be written as

$$T = T_0 + 2q\sqrt{t/\pi\rho ck} \tag{4}$$

where T_0 is initial temperature of FLiLi surface. Ignoring the distance between thermocouple tip and FLiLi surface for the moment, the temperature measured by the thermocouple can be regarded as a proxy for the surface temperature. The heat flux of plasma to FLiLi surface can be assessed by the equation below

$$q = 0.5\Delta T/\,(t/\pi\rho ck)^{0.5}. \tag{5}$$

For FLiLi plate, the main heat sink material is Cu. Hence, ρ, c and k are 8.9×10^3 kg/m^3, 0.39×10^3 J/(kg·°C) and 400 W/(m·K), respectively. Fig. 8 shows the heat flux of FLiLi surface during shot #71355 is trending to rapidly ascend, especially after 5.5 s. The average rate of heat flux on FLiLi surface rise is about 0.15 MW/ (m^2·s). The max heat flux is about 1.3 MW/m^2. Nevertheless, the heat flux of shot #71366 on FLiLi surface rises rapidly than that of shot #71355 at the beginning 5 s, and the heat flux also rose significantly at 5.5 s, but the rate of heat flux increase was reduced when He cooling was used. In general, the heat flux on FLiLi surface tends to be on rise. The max heat flux on FLiLi surface is just about 1.1 MW/m^2. The average rate of heat flux on FLiLi surface rise during shot #71356 is about 0.13 MW/(m^2·s). Although the plasma parameters are identical in shots of #71355 and #71356. However, through comparative of plasma configuration, it's found that the outermost magnetic surface of shot #71356 is about 1.5 mm father than shot #71355 at 5 s, As shown in Fig. 9(a). It means that the plasma

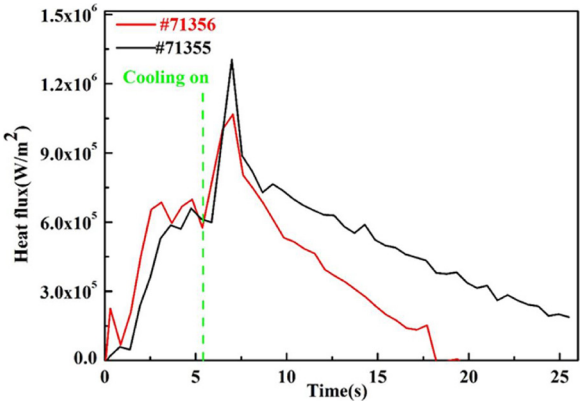

Fig. 8. Heat flux of plasmas on limiter w/o He cooling.

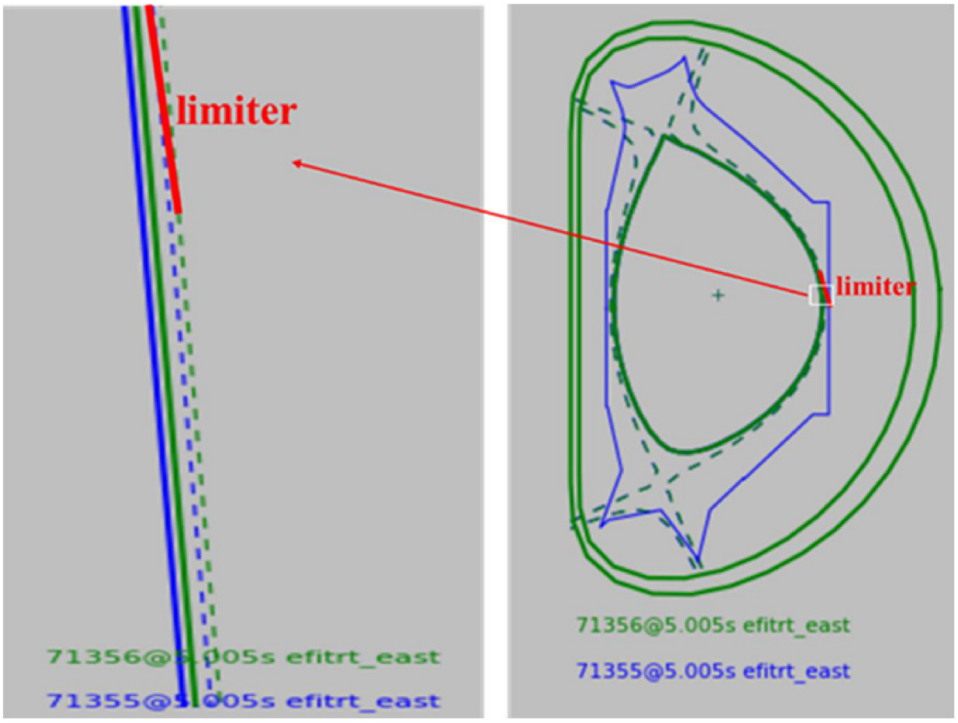

(a)

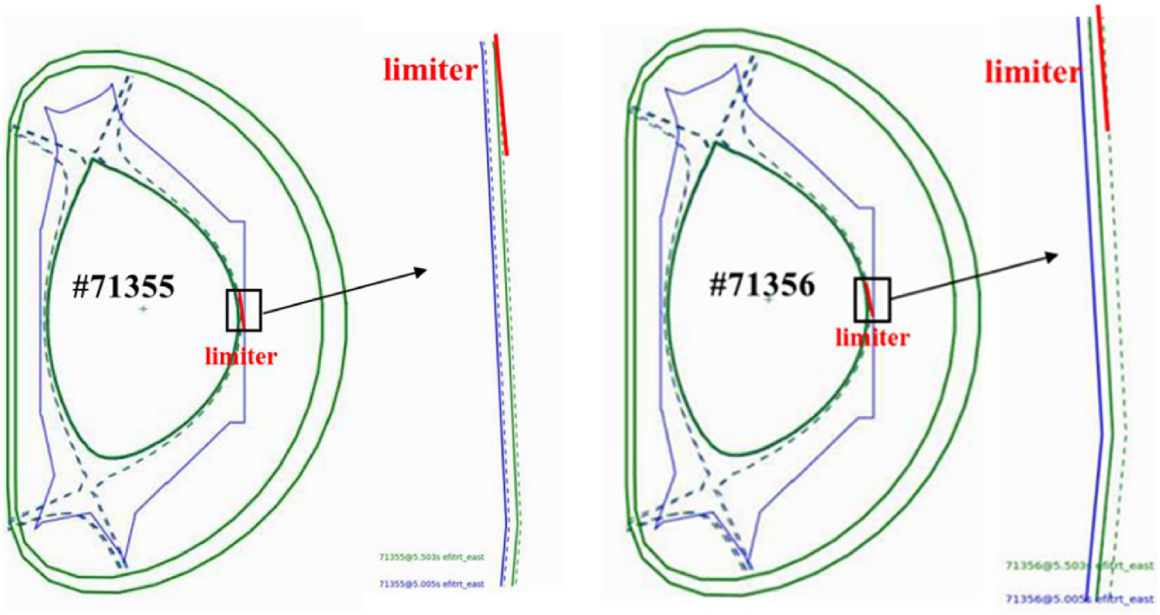

(b)

Fig. 9. Plasma configuration comparison during shots #71355and #71356. Shown are the (a) plasma configuration of shots #71355 and #71356 at 5 s, (b) plasma configuration of shots #71355 and #71356 at 5 s and 5.5 s.

of shot #71356 is closer to FLiLi than shot #71355. Therefore, the heat flux to FLiLi during shot #71356 is higher than that during shot #71355 before 5 s. Moreover, the outermost magnetic surface of shots #71356 and #71355 at 5.5 s is about 2 mm father than that at 5 s, as shown in Fig. 9(b). Therefore, the heat fluxes to FLiLi in the two discharges looks consistent with the time evolutions of plasma parameters at the beginning 5 s, but heat fluxes also increased significantly at ~5.5 s. Finally, by comparing the heat flux of plasmas to FLiLi surface w/o He cooling, it is concluded that the incident heat flux is removed about 0.2 MW/m2 by He cooling. Which is of course beneficial to reduce erosion of FLiLi.

As described in Refs [21–23], a strong rise in Li emission intensity can cause the plasma to disrupt. Several possible reasons for the enhanced Li emission may be sputtering, evaporation, splashing. The rate of evaporation of Li from the open surface of FLiLi into vacuum is determined by [24]:

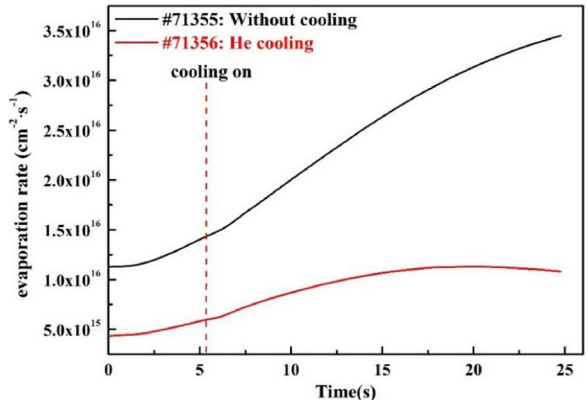

Fig. 10. Evaporation of Li during plasma discharge w/o He cooling.

$$G = 3.09 \times 10^{22} \times \frac{10^{[f-g/T]}}{\sqrt{T}\sqrt{M_{Li}}} \quad (6)$$

where, T and M_{Li} are temperature of limiter and molar mass of Li. The evaporation rate f is 8.0. Constant g, which is the ratio of evaporation heat to Boltzmann constant, is 8143.0 [24]. The Li evaporating capacity for per second on the surface of liquid Li limiter can be calculated by the following formula:

$$N = G \times S, \quad (7)$$

S is the surface area of FLiLi ~ 960 cm^2. From Eqs. (6) and (7) it can be seen that the evaporation rate and evaporating capacity of Li are strong functions of surface temperature. The computed Li evaporation rates on FLiLi as a function of time in the comparison discharges are shown in Fig. 10. The max evaporating capacity of Li during shots #71355 and #71356 are about 3.3×10^{19} and 1.0×10^{19} respectively. Note that the trend of evaporative flux is similar to temperature evolution curves during shots #71355 and #71356. This shows that the He cooling can prevent lots of Li evaporation at some extent by controlling temperature of FLiLi.

The effect of He cooling on FLiLi was also observed during shot #71,357, in which the plasma heating power was increased. Shot #71,357 has similar plasma density and loop voltage with shots #71356 and #71355, but it had higher plasma current ~ 520 kA as compared with 400 kA in the other two discharges Fig. 11(a)). The position of FLiLi was also same as previous two shots. Hence, the Ohmic power of shot #71357 is about 0.12 MW more than that of shot #71356. As shown in Fig. 11(b), the temperature evolution of the FLiLi surface during shot #71357 is similar to that of shot #71356. At the beginning, the surface temperature of FLiLi rises rapidly. Then the temperature increases slowly when He cooling was used. Finally, the temperature flattens rapidly when the max temperature reaches 380 degrees. Thus, compared to the shot of #71355, although the plasma power increased by 0.12 MW, while the max temperature different of the limiter just increased by 1 °, suggesting the He cooling is effective.

Fig. 12 compares the temperature difference of three channels 201, 205 and 209 with and without gas cooling. It is found that the temperature difference of channel 205 during plasma discharges is always higher than that of channels 201 and 209. Because channel 205 is located nearest the main contact region of the hot plasma, a more rapid temperature rises during plasma discharges and a more rapid cool-off with He cooling activated is expected. In addition, the temperature different of channel 201 is always higher than that of channel 209, due to the area near channel 209 is preferentially cooled by the cooler He gas than the region nears channel 201 due to the channel 209 and 201 near gas inlet and gas outlet of the cooling tube respectively. These results are in good agreement with the conceptual cooling design of the FLiLi.

Fig. 13 shows the oxidized surface of FLiLi after the liquid Li

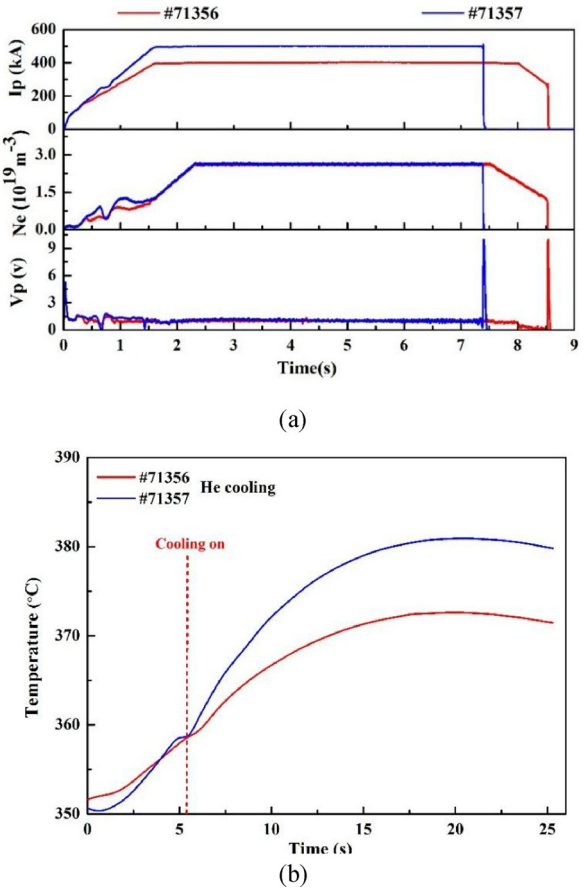

Fig. 11. FLiLi surface temperature during shots #71356 and #71357. Shown are the (a) plasma parameters, (b) FLiLi surface temperature evolution.

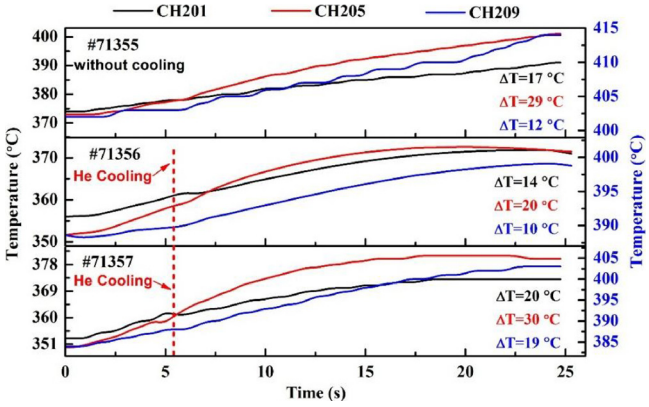

Fig. 12. Temperature difference of channels 201, 205 and 209 during plasma discharges with and without gas cooling.

experiment. It is noted that the liquid Li coverage uniformity on the FLiLi surface increased to > 80 %, as compared to ~30 % in the 2014. Compared to the 2014 campaign, as shown in Fig. 1, the FLiLi surface is relatively flat and there is no severe damage caused by PSI. These results suggest that the real-time gas cooling system may play an important role in protection of FLiLi surface during plasma discharges.

4. Conclusions

Two kinds of gas cooling, He and Ar were tested in FLiLi system before exposure to plasma in EAST. It was found that the cooling performance of He is much better than Ar. Subsequently the real-time He

Fig. 13. FLiLi surface status after exposure to air.

gas cooling has been successfully performed on FLiLi in EAST in 2016. The He cooling could effectively restrain the rapid temperature increase and remove the heat flux to FLiLi surface during plasma discharges. In particular, under the function together with factors of upgraded design and real-time gas cooling to the reduction of the surface temperature, there is no damage to the FLiLi surface after entire plasma discharge sequence. These results provide a conceptual, technical reference for the cooling design of a liquid Li limiter or divertor in future fusion devices.

CRediT authorship contribution statement

X.C. Meng: Investigation, Methodology, Writing - original draft. **M. Huang:** Investigation, Experiment, Methodology, Data curation. **C.L. Li:** Investigation, Visualization. **Z. Sun:** Data curation. **W. Xu:** software. **R. Maingi:** Conceptualization, Writing - review & editing. **K. Tritz:** Conceptualization. **D. Andruczyk:** Conceptualization, Investigation, Writing - review & editing. **Y.Z. Qian:** software. **Q.X. Yang:** Conceptualization, Methodology. **X.L. Yuan:** software, Data curation. **J.J. Huang:** Writing - review & editing. **X. Gao:** Writing - review & editing. **B. Yu:** Writing - review & editing. **J.G. Li:** Conceptualization, Writing - review & editing. **G.Z. Zuo:** Data curation, Investigation, Writing - review & editing, Supervision. **J.S. Hu:** Conceptualization, Writing - review & editing, Supervision.

Declaration of Competing Interest

The authors declare that they have no known competing financial interests or personal relationships that could have appeared to influence the work reported in this paper.

Acknowledgement

This research is funded by National Key Research and Development Program of China (2017YFA04025000 and 2017YFE030110), National Nature Science Foundation of China (11625524, 11775261, 11605246, 119050138, 11905148) and in part by the US Department of Energy under contract DE-AC02-09CH11466. The authors would like to acknowledge the support of Shenzhen Clean Energy Research Institute.

References

[1] G. Federici, C.H. Skinner, J.N. Brooks, et al., Nucl. Fusion. 41 (2001) 1967.
[2] M.A. Jaworski, T. Abrams, J.P. Allain, et al., Nucl. Fusion. 53 (2013) 083032.
[3] R. Majeski, R. Doerner, T. Gray, et al., Phys. Rev. Lett. 97 (2006) 075002.
[4] V.P. Ridolfini, A. Alekseyev, B. Angelini, et al., Nucl. Fusion. 47 (2007) S608.
[5] S.V. Mirnov, E.A. Azizov, V.A. Evtikhin, et al., Plasma Phys. Controlled. Fusio.n 48 (2006) 821.
[6] J.S. Hu, J. Ren, Z. Sun, et al., Fusion Eng. Des. 89 (2014) 2875.
[7] M. Ono, M.A. Jaworski, R. Kaita, et al., Nucl. Fusion. 53 (2013) 113030.
[8] G.Z. Zuo, J. Ren, J.S. Hu, et al., Fusion Eng. Des. 89 (2014) 2845.
[9] J. Ren, G.Z. Zuo, J.S. Hu, et al., Rev. Sci. Instrum. 86 (2015) 023504.
[10] J.S. Hu, G.Z. Zuo, J. Ren, et al., Nucl. Fusion. 56 (2016) 046011.
[11] G.Z. Zuo, J.S. Hu, R. Maingi, et al., Nucl. Fusion. 59 (2019) 016009.
[12] X.C. Meng, C. Xu, G.Z. Zuo, et al., J. Nucl. Mater. 513 (2019) 282.
[13] G.Z. Zuo, J.S. Hu, R. Maingi, et al., Rev. Sci. Instrum. 88 (2017) 123506.
[14] X.L. Yuan, Y. Chen, J.S. Hu, et al., Fusion Eng. Des. 112 (2016) 332.
[15] D. Fang, G.N. Luo, R.A. Pitts, et al., J. Nucl. Mater. 455 (2014) 710.
[16] X.M. You, L.L. Tong, X.W. Cao, et al., Nucl. Sci. Eng. 37 (2017) 374.
[17] D.M. Yao, Y.T. Song, S.T. Wu, et al., Fusion Eng. Des. 69 (2003) 355.
[18] I.E. Lyublinski, A.V. Vertkov, V.A. Evtikhin, et al., Plasma. Devices. Oper 17 (2009) 42.
[19] G. Mazzitelli, M.L. Apicella, A. Alexeyev, et al., Fusion Eng. Des. 86 (2011) 580.
[20] J.P. Allain, D.G. Whyte, J.N. Brooks, Nucl. Fusion. 44 (2004) 655.
[21] Z. Sun, J.S. Hu, G.Z. Zuo, et al., J. Nucl. Mater 438 (2013) S899.
[22] J.S. Hu, G.Z. Zuo, J.G. Li, et al., Fusion Eng. Des. 85 (2010) 930.
[23] G.Z. Zuo, J. Ren, J.S. Hu, et al., Fusion Eng. Des. 89 (2014) 2845.
[24] B.Q. Deng, J.C. Yan, J.H. Huang, Chin. J. Nucl. Sci. Eng. 20 (2000) 373.